

Critical theory of the topological quantum phase transition in the AKLT–SZH chain

Hong-Chen Jiang,¹ Stephan Rachel,² Zheng-Yu Weng,³ Shou-Cheng Zhang,⁴ and Zhenghan Wang¹

¹*Microsoft Research, Station Q, University of California, Santa Barbara, CA 93106*

²*Department of Physics, Yale University, New Haven, CT 06520*

³*Institute for Advanced Study, Tsinghua University, Beijing, 100084, P. R. China*

⁴*Department of Physics, McCullough Building, Stanford University, Stanford, CA 94305*

We systematically study the phase diagram of $S = 2$ spin chain by means of density-matrix renormalization group and exact diagonalization. We confirm the presence of a dimer phase in the AKLT–SZH model and find that the whole phase boundary between dimer and SZH phases, including the multicritical point, is a critical line with central charge $c = 5/2$. Finally, we propose and confirm that this line corresponds to $SO(5)_1$ Wess–Zumino–Witten conformal field theory.

PACS numbers: 05.30.Rt, 75.10.Jm, 75.10.Pq

In recent years, investigations of topological phases and phase transitions has attracted great attention in condensed matter physics¹ and quantum information theory². Topological phases are characterized by a bulk gap separating excitations from the ground state and by the presence of gapless edge modes. A topological phase cannot be deformed continuously into a conventional, topologically trivial phase without going through a phase transition, in which the gap closes and the edge modes merge with the bulk. The quantum Hall state³ and the recently discovered topological insulators¹ are examples of topological states of quantum matter.

Topological phases even appear in one dimensional (1D) systems. The Haldane phase⁴ of integer quantum spin chains is an example of a *symmetry protected topological phase*^{5,6}. In 1987, Affleck, Kennedy, Lieb, and Tasaki (AKLT)⁷ introduced a family of exactly solvable integer spin models with valence bond solid (VBS) ground state and proved that VBS states share the key features of Haldane gap liquids for integer spin chains. The ground state of AKLT model can be exactly formulated in terms of Schwinger bosons⁸, $|\Psi^{\text{AKLT}}\rangle = \prod_{\langle ij \rangle} (a_i^\dagger b_j^\dagger - b_i^\dagger a_j^\dagger)^S |0\rangle$, where S is the local spin. The VBS states are unique ground states of the AKLT Hamiltonian for periodic boundary condition (PBC); for open boundary conditions (OBC), however, the ground state is $(S+1)^2$ -fold degenerate with edge spins $S/2$. The parent Hamiltonian for the VBS states $|\Psi^{\text{AKLT}}\rangle$, here for $S = 2$, is conveniently defined in terms of projection operators⁷,

$$H^{\text{AKLT}} = \sum_{\langle ij \rangle} K_3 P_3(i, j) + K_4 P_4(i, j), \quad (1)$$

where $K_3, K_4 > 0$ and P_3 and P_4 project onto the spin 3 and spin 4 subspaces at the bond (i, j) , respectively. The edge spin is boson-like $S = 1$ and the square of the time reversal operator T satisfies $T^2 = 1$.

In 1998, Scalapino, Zhang, and Hanke (SZH) introduced an $SO(5)$ symmetric superspin model⁹ with an exact VBS ground state. The local spin in the SZH model transform under the five-dimensional vector representation of $SO(5)$. SZH presented an exact ground state wave function expressed as a matrix product state of Dirac Γ

matrices, and showed that the ground state is 16-fold degenerate for OBC. This model can be naturally mapped onto a spin 2 chain, with fermion-like $S = 3/2$ edge spin¹⁰ and $T^2 = -1$. Following SZH's work, more VBS states with higher symmetry groups have been constructed^{11,12}.

The ground state of SZH model is given by $|\Psi^{\text{SZH}}\rangle = \sum_{\{m_i\}} \text{Tr}(\Gamma^{m_1} \Gamma^{m_2} \dots \Gamma^{m_N}) |m_1 \dots m_N\rangle$, where the Γ^m fulfill $\Gamma^a \Gamma^b = 2\delta^{ab} + 2i\Gamma^{ab}$ and m_i is a vector label of the $SO(5)$ group, which can also be interpreted as the $m_i = -2, -1, 0, 1, 2$ quantum numbers of spin 2. The corresponding Hamiltonian is given by

$$H^{\text{SZH}} = \sum_{\langle ij \rangle} J_2 P_2(i, j) + J_4 P_4(i, j), \quad (2)$$

where $J_2, J_4 > 0$ and P_2 and P_4 again are the $SU(2)$ bond projection operators onto spin 2 and 4, respectively. The ground state is unchanged up to an $SO(5)$ rotation.

Like for topological insulators, the bulk topology is related to the edge states of an open chain. Consequently, AKLT and SZH models describe different topological phases. As recently pointed out¹³, odd integer spin AKLT models are protected by a couple of symmetries, *e.g.* time reversal, while even integer spin AKLT models are solely protected by global $SU(2)$ symmetry. Since the first case is characterized by half-integer edge spin, the SZH model is similar to odd spin AKLT models (notice that the spin 3 AKLT model exhibits an edge spin $3/2$ like SZH). Both, the AKLT and SZH phases are thus protected by symmetries, but the SZH phase seems to be much more robust. Given the topological distinction of the two ground states, we construct a model Hamiltonian interpolating between the AKLT and SZH models:

$$\begin{aligned} H(\alpha) &= (1 - \alpha) H^{\text{AKLT}} + \alpha H^{\text{SZH}} \\ &= \sum_{\langle ij \rangle} [\alpha P_2(i, j) + (1 - \alpha) P_3(i, j) + \beta P_4(i, j)]. \end{aligned} \quad (3)$$

Here, we set $J_2 = K_3 = 1$, $J_4 = K_4 = \beta$. As the edge state is robust unless the gap closes, there must exist one or several topological quantum phase transitions (TQPT) when varying α from 0 to 1.

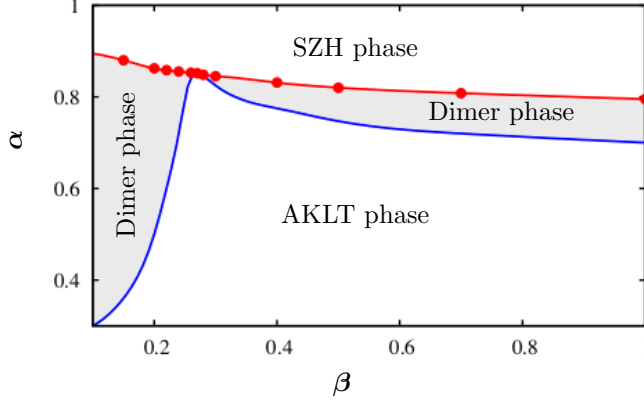


FIG. 1: (color online) Ground state phase diagram of the Hamiltonian (3) obtained by DMRG with $N = 600$ sites. The location of second order phase transition is indicated by the red line. The region above the red line belongs to SZH phase, while the region below the dashed blue line belongs to AKLT phase. The intermediate regime between the topologically different SZH and AKLT phases are dimer phases.

In Ref.14, the ground state phase diagram of the AKLT-SZH model (3) has been studied by means of density-matrix renormalization group (DMRG)¹⁵. Between the AKLT and SZH phases, a possible dimer phase has been found. The most interesting feature is the presence of a multicritical (MC) point, at which a direct TQPT occurs between the two distinct phases. However, there are still some important questions. (1) Does the dimer phase indeed exist in the thermodynamic limit? (2) What is the phase diagram for $\beta < 0.27$? (3) What is the central charge and low-energy effective theory at the MC point? (4) Does the effective theory spread over the whole phase boundary?

Motivated by these questions, in this paper we will revisit the model (3) and try to answer all open questions. For the present study, we keep up to $m = 3400$ DMRG states with more than 16 sweeps to get converged results, and the truncation error is less than 10^{-9} . We use both OBC and PBC with system sizes up to $N = 600$ sites.

Dimer order parameter. We confirm the presence of the dimer phase for $\beta > 0.27$, see the phase diagram Fig. 1. In addition, we find a much larger dimer phase for $\beta < 0.27$. To clarify the presence of the dimer phase, we have calculated the dimer order parameter (DOP), $\mathcal{D} = |\langle \mathbf{S}_i \mathbf{S}_{i+1} \rangle - \langle \mathbf{S}_{i+1} \mathbf{S}_{i+2} \rangle|$, as a function of α and β , where $i = N/2$ and we imposed OBC. In Fig. 2(a), exemplarily the DOP as a function of α at $\beta = 0.2$ for different system sizes is shown. In the inset, the finite-size scaling is also performed to obtain the DOP in the thermodynamic limit. As shown in Figs. 1 and 2, when β decreases from $\beta = 1$, also the maximum amplitude of DOP decreases, and the dimer phase shrinks with α monotonously. Finally, at the MC point $\beta = 0.27$, the DOP vanishes for any α . Surprisingly, for smaller values of β there is a revival of the dimer phase, which be-

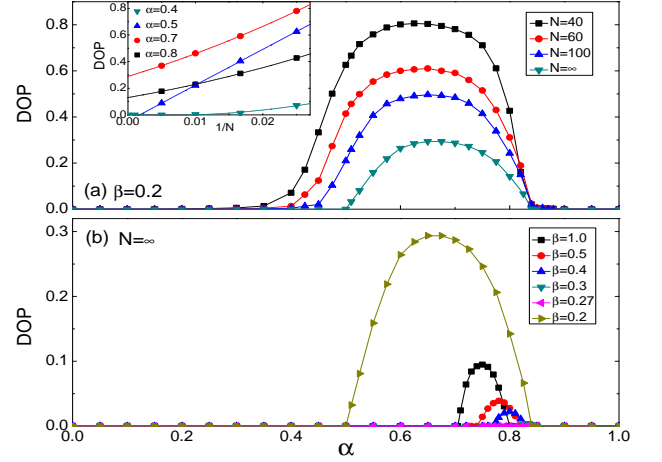


FIG. 2: (color online) Dimer order parameters (DOP) of the Hamiltonian (3) with different of α and β . (a) DOP for $\beta = 0.2$ at system size $N = 40, 60$ and 100 , as well as in the thermodynamic limit $N = \infty$. The finite-size scaling is given in the inset. (b) DOP for different β , which disappears at the multi-critical point $\beta = 0.27$.

comes even larger and the magnitude of DOP increases, indicating a very robust dimer phase at small β region. In the limit $\beta = 0$, the P_4 term vanishes and we expect a huge ground state degeneracy. Therefore, it will be extremely difficult to get converged DMRG results and we only consider $\beta \geq 0.1$ in the phase diagram Fig. 1. Like for the general spin 1 chain, we expect a *generic* dimer phase containing the Hamiltonian $H_{\text{dimer}} = \sum_i -P_0(i, i+1)$ with an enhanced $\text{SU}(5)$ symmetry. We performed DMRG calculations to verify this guess. We also studied the two Hamiltonians interpolating between H_{dimer} and the dimer phase for $\beta > 0.27$ and for $\beta < 0.27$, respectively. In both cases, we found in the second derivative of the ground state energy with respect to the interpolation parameter a signal for a second order phase transition. So it might be that the general spin 2 chain contains three different dimer phases. The nature of the phase transition between dimer and AKLT phases seems to be a higher order (*i.e.*, third or more) phase transition. Therefore, it will be extremely difficult to locate the exact phase boundary numerically.

String order parameter. To distinguish different topological phases, one way is to use the hidden string order parameter (SOP) defined as $\mathcal{G}(\theta) = \langle \hat{A}_i \exp(i\theta \sum_{k=i}^{j-1} \hat{A}_k) \hat{A}_j \rangle$. For spin- S AKLT model, the peak of SOP is at $\theta_c = \pi/S$ for $\hat{A}_i = S_i^z$. But this SOP cannot be used to distinguish the AKLT and SZH phase since it is finite in both phases. Fortunately, Tu *et al.*¹⁰ proposed a SOP with $\hat{A}_i = \frac{1}{6}(S_i^z)[(S_i^z)^2 - 1]$ and $\theta_c = \pi$ which *knows* about $\text{SO}(5)$ symmetry of the SZH model and which is finite only in the SZH phase. Therefore, we can use the SOP to characterize the TQPT between SZH and other phases (in addition to $d^2E/d\alpha^2$).

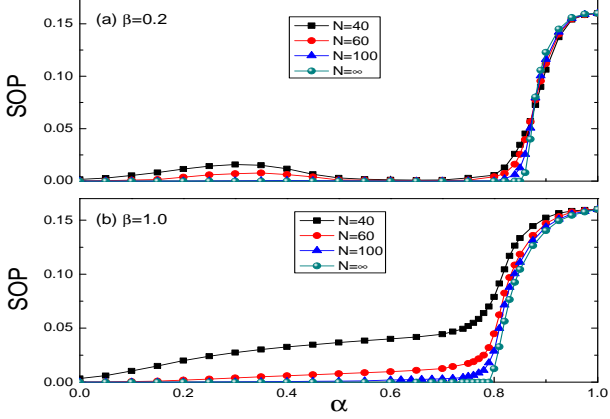


FIG. 3: (color online) String order parameters of $H(\alpha)$ for (a) $\beta = 0.2$ and (b) $\beta = 1.0$, for system size $N = 40, 60$ and 100 , and the extrapolated value for $N = \infty$.

In Fig. 3, the SOP for $\beta = 0.2$ and $\beta = 1.0$ is shown for several system sizes and for $N \rightarrow \infty$. In both the AKLT and dimer phase, $\mathcal{G}(\pi) \rightarrow 0$. In the SZH phase, however, $\mathcal{G}(\pi)$ remains finite, and approaches its maximum value¹⁰ $4/5^2 = 0.16$ in the SZH limit $\alpha = 1$.

Entanglement spectrum. To identify different phases, we can also use the entanglement spectrum (ES), which was originally introduced by Haldane¹⁶ in the context of FQHE and later applied to spin chains in a momentum basis¹⁷. The ES is defined as the set of eigenvalues of the reduced density matrix $\rho_A \equiv \text{Tr}_B |\Psi\rangle\langle\Psi|$, with A being a subsystem and B the remainder of the system. Here we use the real space ES with PBC to characterize the different phases. As shown in Fig. 4, the lowest level of ES in AKLT phase is 9-fold degenerate, this degeneracy is associated with the edge spin 1. By increasing α , a finite size splitting of the 9 ground states occurs (chain length $N = 100$). After entering the dimer phase, the lowest value of the ES becomes non-degenerate. By further increasing α , the system enters the SZH phase, the lowest level of the ES becomes degenerate again, but now the degeneracy is 16-fold in agreement with edge spin $3/2$. In all the three phases, the lowest level of ES is separated by a large gap from the other levels.

Central charge. The most interesting feature is the presence of the MC point, as shown in Fig. 1. To characterize the critical theory we should determine central charge and scaling dimensions. The central charge can be obtained by calculating the von Neumann entropy of a subsystem A with length x , defined as $S^{\text{vN}} = -\text{Tr}(\rho_A \ln \rho_A)$. For critical systems, it has been established¹⁸ that $S^{\text{vN}} = (c/3) \ln(x') + \tilde{c}_1$ for PBC, and $S^{\text{vN}} = (c/6) \ln(2x') + \ln(g) + \tilde{c}_1/2$ for OBC, where c is the central charge of the conformal field theory (CFT), \tilde{c}_1 is a model dependent constant, and g is Affleck and Ludwig's universal boundary term¹⁹. For finite chains, we can use

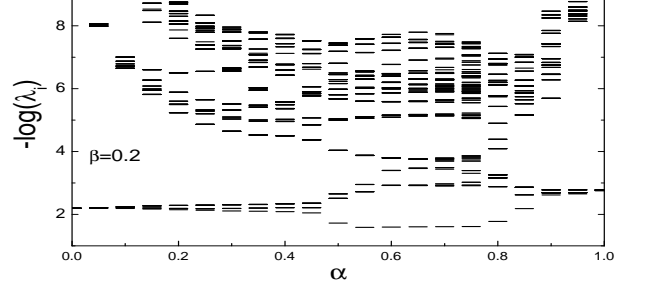


FIG. 4: The 100 lowest levels of the entanglement spectrum $-\log \lambda_i$ for system size $N = 100$ at $\beta = 0.2$. λ_i are the eigenvalues of the reduced density matrix.

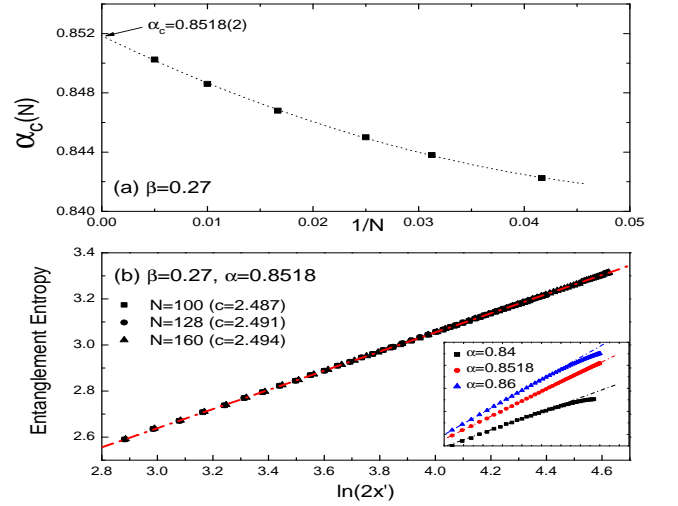


FIG. 5: (color online) (a) Finite-size scaling of the peak position $\alpha_c(N)$ of $d^2E/d\alpha^2$ as a function of α at $\beta = 0.27$. (b) Von Neumann entropy S^{vN} at the multi-critical point for different chain length with the fitted central charge c . Inset: S^{vN} for different parameter points is shown for comparison.

the conformal mapping $x \rightarrow x' = (N/\pi) \sin(\pi x/N)$. Using this formula the central charge can be extracted in excellent agreement with the CFT prediction^{20,21}.

By performing finite-size scaling of the peak position of $d^2E/d\alpha^2$ as a function of β and α , we find the exact position of the MC point at $(\beta_c, \alpha_c) = (0.27, 0.8518)$. In Fig. 5(a), the finite-size scaling is shown for $\beta = 0.27$. In Fig. 5(b), we show S^{vN} at the MC point for different system sizes. The regression fit for S^{vN} shows very good convergence with system size, indicating a central charge $c = 5/2$. For comparison, in the inset of Fig. 5(b), we show the results for some points away from the MC point where S^{vN} starts to saturate indicating the opening of a gap. In the same way, we find $c = 5/2$ for the whole critical line between SZH and dimer phases.

Effective field theory. To find the corresponding CFT,

TABLE I: List of CFT with central charge $c = 5/2$. S_2/S_1 is the ratio of the second and first primary scaling dimensions.

	$\text{SO}(5)_1$	$\text{SU}(2)_{10}$	$\text{SU}(2)_2 \times \text{U}(1)$	$\text{SU}(2)_4 \times \text{Ising}$	MC
$\frac{S_2}{S_1}$	1.6	2.67	2.67	2.67	1.56

we have listed all the simple corresponding candidates with central charge $c = 5/2$ in Table I. S_2/S_1 is the ratio between the scaling dimensions of the second and first non-trivial primary fields. To characterize the CFT theory at the critical line, we rescale and match the lowest three finite-size energy levels obtained numerically by exact diagonalization (ED) for systems with up to $L = 12$ sites to the form of the spectrum of a CFT²²,

$$E(L) = E_1 L + \frac{2\pi v}{L} \left(-\frac{c}{12} + h + \bar{h} \right). \quad (4)$$

Here the velocity v is an overall non-universal scale factor and the scaling dimensions $h + \bar{h}$ take the form $h = h^0 + n, \bar{h} = \bar{h}^0 + \bar{n}$, with n and \bar{n} non-negative integers. h^0 and \bar{h}^0 are the holomorphic and antiholomorphic conformal weights of primary fields in the CFT. The momenta (in units $2\pi/L$) are such that $k = h - \bar{h}$ or $k = h - \bar{h} + L/2$. We consider the energy spectrum at $k = 0$ with scaling dimension $S = 2h$ (*i.e.*, $h = \bar{h}$). We find that $S_2/S_1 = 1.56$ at the critical line. Comparing this value with the values in Table I, we find that only $\text{SO}(5)_1$ is compatible with our data, while all the other candidates can be explicitly ruled out. To further confirm this, we also calculate the ratio $(1 + S_2)/(1 + S_1)$ at

$k = 2\pi/L$. We find $(1 + S_2)/(1 + S_1) = 1.27$, which is also consistent with the value $(1 + 1)/(1 + 5/8) = 1.23$ (here $n = 1$) of $\text{SO}(5)_1$ CFT, by considering the finite-size effect. We conclude that the critical line is described by $\text{SO}(5)_1$ Wess–Zumino–Witten (WZW) model.

This result is particularly interesting since we expect three integrable models in the phase diagram of the general spin 2 chain²³: the Takhtajan–Babujian chain ($\text{SU}(2)_4$ WZW with $c = 2$), the permutation operator ($\text{SU}(5)_1$ WZW with $c = 4$), and the *Reshetikhin* model. From the latter model it is believed that it could be described by $\text{SO}(5)_1$ WZW with $c = 5/2$ ²⁴. It turns out that this model is located near our critical line in the phase diagram of the general spin 2 chain. Indeed we find $c = 5/2$ for the Reshetikhin model, but we leave its connection to our critical line as an open question²⁴.

In conclusion, we have confirmed the phase diagram of the AKLT–SZH chain; remarkably, also for $\beta < 0.27$ a dimer phase is present. The critical line separating the SZH and dimer phases has the same central charge $c = 5/2$ and can be described by $\text{SO}(5)_1$ WZW theory.

Acknowledgement. We thank S. Trebst, L. Balents, Z. C. Gu, S. Capponi, B. A. Bernevig, A. Läuchli, and R. Thomale for insightful discussions. We thank C. K. Xu for pointing out to us the possibility of $\text{SO}(5)_1$ theory. HCJ thanks D. N. Sheng for great help on ED results. HCJ acknowledges funding from Microsoft Station Q. SCZ is supported by the NSF under grant numbers DMR-0904264, SR by the DFG under Grant No. RA 1949/1-1, and ZYW by NSFC and NPBR grants of MOST.

-
- ¹ X.-L. Qi and S.-C. Zhang, Phys. Today **63**(1), 33 (2010).
² A. Kitaev, Ann. Phys. (N.Y.) **321**, 2 (2006).
³ K. v. Klitzing, G. Dorda, and M. Pepper, Phys. Rev. Lett. **45**, 494 (1980).
⁴ F. D. M. Haldane, Phys. Rev. Lett. **50**, 1153 (1983).
⁵ Z. C. Gu and X. G. Wen, Phys. Rev. B **80**, 155131 (2009).
⁶ F. Pollmann, A. M. Turner, E. Berg, and M. Oshikawa, Phys. Rev. B **81**, 064439 (2010).
⁷ I. Affleck, T. Kennedy, E. H. Lieb, and H. Tasaki, Phys. Rev. Lett. **59**, 799 (1987); *ibid*, Commun. Math. Phys. **115**, 477 (1988).
⁸ D. P. Arovas, A. Auerbach, and F. D. M. Haldane, Phys. Rev. Lett. **60**, 531 (1988).
⁹ D. Scalapino, S.-C. Zhang, and W. Hanke, Phys. Rev. B **58**, 443 (1998).
¹⁰ H. H. Tu, G. M. Zhang, and T. Xiang, Phys. Rev. B **78**, 094404 (2008); *ibid*, J. Phys. A: **41**, 415201 (2008).
¹¹ A. Klümper, A. Schadschneider, and J. Zittartz, J. Phys. A **24**, L955 (1991); I. Affleck, D. P. Arovas, J. Marston, and D. Rabson, Nucl. Phys. B **366**, 467 (1991); D. Schuricht and S. Rachel, Phys. Rev. B **78**, 014430 (2008); S. Rachel, EPL **86**, 37005 (2009); D. P. Arovas, K. Hasebe, X.-L. Qi, S.-C. Zhang, Phys. Rev. B **79**, 224404 (2009); H. H. Tu, G. M. Zhang, T. Xiang, Z. X. Liu, and T. K. Ng, Phys. Rev. B **80**, 014401 (2009).
¹² D. Zheng, G. M. Zhang, T. Xiang, and D. H. Lee, arXiv:1002.0171.
¹³ F. Pollmann, E. Berg, A. M. Turner, and M. Oshikawa, arXiv:0909.4059.
¹⁴ J. D. Zang, H. C. Jiang, Z. Y. Weng, and S. C. Zhang, Phys. Rev. B **81**, 224430 (2010).
¹⁵ S. R. White, Phys. Rev. Lett. **69**, 2863 (1992).
¹⁶ H. Li and F. D. M. Haldane, Phys. Rev. Lett. **101**, 010504 (2008).
¹⁷ R. Thomale, D. P. Arovas, and B. A. Bernevig, Phys. Rev. Lett. **105**, 116805 (2010).
¹⁸ P. Calabrese and J. Cardy, J. Stat. Mech. (2004) P06002.
¹⁹ I. Affleck and A. W. W. Ludwig, Phys. Rev. Lett. **67**, 161 (1991).
²⁰ M. Fühlinger, S. Rachel, R. Thomale, M. Greiter, and P. Schmitteckert, Ann. Phys. (Berlin) **17**, 922 (2008).
²¹ C. Gils, S. Trebst, A. Kitaev, A. W. W. Ludwig, M. Troyer, Z. Wang, Nature Physics **5**, 834 (2009).
²² J. Cardy, Nucl. Phys. B **270**, 186 (1986).
²³ T. Kennedy, J. Phys. A: Math. Gen. **25**, 2809 (1992).
²⁴ H. H. Lin, L. Balents, and M. P. A. Fisher, Phys. Rev. B **58**, 1794 (1998); P. Bouwknegt and K. Schoutens, Phys. Rev. Lett. **82**, 2757 (1999); F. Alet, S. Capponi, H. Nonne, P. Lecheminant, and I. P. McCulloch, arXiv:1011.1265.